The Interaction of Specific Peptide Aptamers With the DNA Binding Domain and the Dimerization Domain of the Transcription Factor Stat3 Inhibits Transactivation and Induces Apoptosis in Tumor Cells

Kerstin Nagel-Wolfrum,[1] Claudia Buerger,[1] Ilka Wittig,[1] Karin Butz,[2] Felix Hoppe-Seyler,[2] and Bernd Groner[1]

[1]Georg-Speyer-Haus, Institute for Biomedical Research, Frankfurt am Main, Germany and [2]Angewandte Tumorvirologie, Deutsches Krebsforschungszentrum, Heidelberg, Germany

Abstract

The transcription factor signal transducer and activator of transcription (Stat) 3 is activated through the interleukin-6 family of cytokines and by binding of growth factors to the epidermal growth factor (EGF) receptor. It plays an essential role in embryonic development and assumes specialized tasks in many differentiated tissues. Constitutively activated Stat3 has been found in tumor cell lines and primary tumors and plays a crucial role in tumor cell survival and proliferation. To inhibit the oncogenic action of Stat3 in tumor cells, we have selected short peptides, so-called peptide aptamers, which specifically interact with defined functional domains of this transcription factor. The peptide aptamers were selected from a peptide library of high complexity by an adaptation of the yeast two-hybrid procedure. Peptide aptamers specifically interacting with the Stat3 dimerization domain caused inhibition of DNA binding activity and suppression of transactivation by Stat3 in EGF-responsive cells. Similarly, a peptide aptamer selected for its ability to recognize the Stat3 DNA binding domain inhibited DNA binding and transactivation by Stat3 following EGF stimulation of cells. Peptide aptamers were expressed in bacteria as fusion proteins with a protein transduction domain and introduced into human myeloma cells. This resulted in dose-dependent growth inhibition, down-regulation of Bcl-x_L expression, and induction of apoptosis. The inhibition of Stat3 functions through the interaction with peptide aptamers counteracts the transformed phenotype and could become useful in targeted tumor therapy.

Received 9/9/03; revised 1/28/04; accepted 2/5/04.
Grant support: Deutsche Krebshilfe, Dr. Mildred Scheel Stiftung für Krebsforschung, Bonn (10-1626-Gr2), and Novartis Stiftung für Therapeutische Forschung.
The costs of publication of this article were defrayed in part by the payment of page charges. This article must therefore be hereby marked advertisement in accordance with 18 U.S.C. Section 1734 solely to indicate this fact.
Requests for reprints: Bernd Groner, Georg-Speyer-Haus, Institute for Biomedical Research, Paul-Ehrlich-Strasse, 42 D-60596 Frankfurt am Main, Germany. Phone: 49-69-63395180; Fax: 49-69-63395185.
E-mail: groner@em.uni-frankurt.de

Introduction

Insights into the molecular mechanisms underlying the initiation and progression of tumor cells have increased enormously over the past years. Many signaling components have been identified which are mutated or aberrantly expressed in tumor cells when compared with normal cells (1). Such molecules and the signaling pathways affected provide new targets for therapeutic intervention. Signaling molecules, mainly growth factors receptors with intrinsic tyrosine kinase activity or cytoplasmic protein kinases, have been successfully targeted (2–4).

Signaling components with other functions (*e.g.*, transcription factors) have also been taken into consideration as potential targets for cancer drug development. Signal transducer and activator of transcription (Stat) molecules fall into this category. Although their activated forms are found in tumor cells and some of their functional roles in the transformation process have been shown, it has proven difficult to exploit them as targets for therapeutic intervention (5).

Stats are signaling molecules with dual functions: they transmit signals from the cell surface to the nucleus and they directly participate in gene regulation by binding to response elements in gene promoters affecting transactivation (6). As intracellular effectors of growth factors and cytokines, Stat proteins function in the control of proliferation, differentiation, and apoptosis (7–9). On binding of cytokines to cognate receptors, they cause the activation of the receptor, associated Jak kinases, and latent Stat molecules by tyrosine phosphorylation. Phosphorylated Stats dimerize and translocate to the nucleus where they induce gene expression (6). The dual function is reflected in the domain structure of the Stat molecules (Fig. 1A). Dimer formation is mediated by the interaction of the SH2 domain of one Stat molecule with the phosphotyrosine 705 residue on the other subunit. The cooperative binding domain, the DNA binding domain (DBD), and the transactivation domain are necessary to fulfill the functions of the transcription factor.

Constitutive activation of Stat proteins, mainly Stat3 and Stat5, has been found in several tumor cell lines and primary human tumors. These include blood malignancies (leukemias, lymphomas, and multiple myeloma) and tumors of solid tissues (head and neck, breast, and melanoma; Refs. 10, 11). It has been suggested that Stat3 acts as an oncogene (12). Constitutively activated Stat3 signaling participates in the

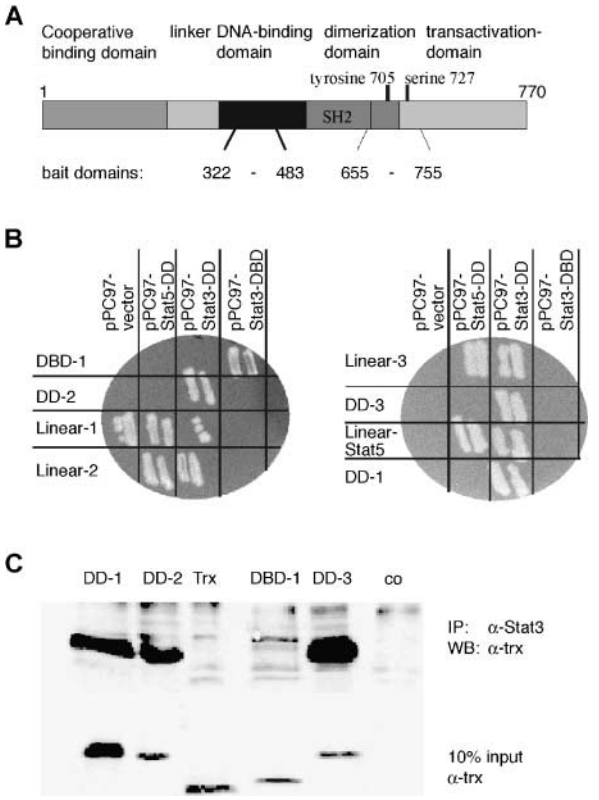

FIGURE 1. Interaction of isolated peptide aptamers with Stat3. **A.** Functional domains of the Stat3 molecule, the cooperative binding domain, the DNA binding domain, and the transactivation domain are indicated. Phosphorylation of the tyrosine 705 in the dimerization region mediates interaction with the SH2 domain of another monomer and causes Stat3 dimer formation. Tyrosine 705 and serine 727 are key phosphorylation sites. Domains used as bait constructs in the yeast two-hybrid screens are indicated. **B.** Isolated peptide aptamers interact specifically with corresponding bait constructs. Empty bait vector (*pPC97*) or bait constructs (*pPC97-Stat5-DD*, *pPC97-Stat3-DD*, and *pPC97-Stat3-DBD*) were transformed in haploid yeast strain PJ69α and mated with haploid yeast strain PJ69a expressing indicated peptide aptamers. Interaction of bait and prey was monitored under selection conditions. **C.** *In vitro* interaction of selected peptide aptamers with full-length Stat3. Whole cell extracts of RPMI 8226 cells were preincubated with recombinant expressed peptide aptamers prior to incubation with anti-Stat3 antibodies and Sepharose A beads. After removing unbound peptide aptamers, samples were subjected to SDS-PAGE, and retained peptide aptamers in the complex were visualized by Western blotting with an anti-Trx antibody.

development and progression of human tumors by prevention of apoptosis and induction of proliferation (9–11). Inhibition studies of Stat3 have shown that the function of the molecule can be down-regulated through Stat3-specific antisense oligonucleotides (13), small interference RNA[3], peptidomimetics (14, 15), dominant-negative Stat3 variants (16–19), and the small molecule inhibitor JSI-124 (20). Down-regulation of Stat function can cause growth arrest and induction of apoptosis in various tumor cells (17, 19–21). The antiapoptotic role of Stat3 has been associated with the down-regulation of the proapoptotic proteins CD95 (Fas and Apo) and tumor necrosis factor-related apoptosis-inducing ligand (TRAIL; Refs. 21, 22) and the up-regulation of antiapoptotic proteins Bcl-x_L and Mcl-1 (16, 23).

New therapeutic strategies are currently being developed which might allow the manipulation of specific gene expression in cancer cells without the transfer of genetic material and the inherent limitations of gene therapy. Proteins and peptides have been tested in animal models for this purpose (24–26). The delivery of peptides and proteins into cells can be mediated by protein transduction domains (PTDs). PTDs cause the rapid internalization of cargo proteins into a wide variety of cell types *in vitro* and *in vivo* by mediating the translocation from the extracellular space through cell membranes (27–30). The delivered cargo allows the manipulation of distinct signal transduction pathways in a dose- and time-dependent fashion (31–34). The utilization of PTD fusion proteins is a most promising strategy for the development of protein therapeutics and has demonstrated its value in preclinical animal models (25, 35).

We have investigated the potential of small peptides with specific binding ability to predetermined domains of Stat3 to interfere with the distinct functional properties of the molecule. For this purpose, we have selected peptide aptamers that recognize either the Stat3-DBD or the Stat3 dimerization domain (DD). To identify peptide aptamers interacting with Stat3, we made use of the yeast two-hybrid selection system. Peptide aptamers were selected from a high complexity library of random 20-mers integrated into the active site loop of the *Escherichia coli* thioredoxin A (Trx) protein (36). Using Trx as a scaffold, the integrated peptide is exposed in a constrained conformation (37). Constrained peptides have substantially higher binding affinities than linear peptides, hydrophobic amino acids can be presented on the outside of the molecule, and the preferred conformation of the constrained peptides should be helpful in determining their crystal structure as a prerequisite for drug design (37–39). Several examples have been described in which specific peptide aptamers were selected and shown to be able to interfere with protein functions and cellular phenotypes (36, 40–45).

In the present study, specific peptide aptamers for the Stat3-DD and the Stat3-DBD were selected in yeast cells. NIH3T3/EGFR (Herc) cells were used to test the effect of the selected peptide aptamers on Stat3 activation following epidermal growth factor (EGF) treatment *in vivo*. Herc cells respond to EGF stimulation with phosphorylation of the EGF receptor (EGFR) and subsequently activate downstream targets like Stat3 and mitogen-activated protein kinase (MAPK) p42/p44. Transient transfection of Herc cells with peptide aptamer expression constructs showed that the selected aptamers are able to interfere with Stat3 function. The effects of the peptide aptamers were further analyzed in two tumor cell lines, the human myeloma U266 cells and the murine melanoma B16 cells. Both cell lines express constitutively active Stat3. Whereas the activating kinase in B16 cells is unknown, in human U266 myeloma cells, the interleukin-6/Jak/Stat3 signaling pathway plays a crucial role in the regulation of cell cycle progression and prevention of apoptosis (46). Blocking Stat3 function in these tumor cells induces apoptosis (16, 17, 21). In present study, in transfection and transduction

[3] K. Dutine, C. Shemanko, N. Castro-Palomino Laria, K. Nagel-Wolfrum, and B. Groner. Downregulation of Stat3 and Stat5 by siRNA in tumor cells, manuscript in preparation.

experiments, one peptide aptamer caused induction of apoptosis in both tumor cell lines tested. These studies show that bifunctional recombinant proteins are suited to specifically interfere with oncogene signaling in tumor cells.

Results

Isolation of Stat3-Interacting Peptide Aptamers

The well-known activation pathway and the corresponding domain structure of Stat3 suggest several strategies for targeted inhibition. In addition to the prevention of phosphorylation of tyrosine 705 by the Jak kinase, it is conceivable to target the dimerization or the DNA binding function of the molecule (10). Our aim is the interference with these functions through small peptides, which specifically recognize appropriate domains of Stat3. For this purpose, a modified yeast two-hybrid system was used. We derived two bait constructs and screened a high complexity peptide aptamer library in yeast. One bait construct comprises part of the Stat3-DD (amino acid positions 655–755; Fig. 1A). This sequence contains the crucial tyrosine 705, which is phosphorylated on activation of Stat3 (47). The second bait comprises part of the Stat3-DBD (amino acid positions 322–483) involved in the binding to promoter regions of Stat3 target genes (Fig. 1A; Ref. 48). Both constructs were fused to a GAL4-DBD.

Both bait constructs were expressed in yeast cells, which were subsequently transformed with expression vectors encoding the random peptide library. The randomized sequences of the peptide library were integrated into the bacterial Trx sequence and fused to the GAL4-TAD (36). The screens were performed in the yeast strain KF-1, which contains three selectable growth markers (Ade2, His3, and Ura3) under the control of three different GAL4 promoter regions (36). In screens using the bait Stat3-DD, yeast clones (2×10^7) were analyzed for their ability to grow in the absence of adenine, uracil, and histidine. Six different transformants were able to grow under selective conditions. Sequence analyses revealed insert sizes of 42 amino acids in three of the isolated clones,

DD-1: PPLVCIRSWCPLMVPHSADLGPASQWLCHRVA SIALLPRYSS
DD-2: VGWTWMSVLVCCDGSGLVPEGPVVVQAG GAVPISGSVALMTD
DD-3: SPISIPIGFVVRHCALHMAVGPLSWPARVSGYS FALEVLTNF

indicating that two peptide aptamer sequences were integrated into the Trx. Three clones were isolated with stop codons localized within the peptide aptamer sequences, resulting in the expression of linear peptides. In screens with the bait construct Stat3-DBD, only one clone (DBD-1: PLTAVFWLIYVLAKAL-VTVC) was selected. The sequence analysis of this peptide aptamer revealed a 20-mer amino acid insert. Blast searches with all identified peptide aptamer inserts revealed no sequence similarities with known proteins.

To confirm the interaction specificity of the selected peptide aptamers and their target domains within the Stat3 molecule, mating experiments were performed. The haploid PJ69a yeast strain was transformed with peptide aptamer expression plasmids and the haploid PJ69α strain was transformed with four different bait constructs as indicated in Fig. 1B. Overnight coculture of the haploid yeast strains resulted in diploid yeast cells, which express the peptide aptamer and the bait construct. Interaction of the peptide aptamer and the bait construct was monitored under selective conditions. Peptide aptamer DD-1 interacted specifically with the bait construct Stat3-DD derived from the Stat3-DD molecule and supported the growth of the diploid yeast cells in selection medium. Binding specificity was also verified for peptide aptamers DD-2 and DD-3 (Fig. 1B). Peptide aptamer DBD-1 obtained in a screen with the Stat3-DBD grew only in the presence of the bait construct Stat3-DBD (Fig. 1B). No unspecific interactions of the peptide aptamers with empty bait vector (pPC97) or bait Stat5-DD, which contained sequences derived from the Stat5-DD (amino acid positions 644–744), were observed. The bait construct Stat3-DBD for peptide aptamers DD-1 to DD-3 and the bait construct Stat3-DD for peptide aptamer DBD-1 were included as additional negative controls. Constructs with stop codons within the peptide aptamers sequence (linear 1 and linear 2) showed unspecific interaction with unrelated bait constructs. Due to their unspecific binding, these linear peptides were not analyzed further. Peptide aptamers DD-1 to DD-3 and DBD-1 were used for further analyses.

Selected Peptide Aptamers Interact With Native Stat3 in Vitro

To confirm the interaction of the selected peptide aptamers with cellular Stat3, coimmunoprecipitation experiments were performed. Peptide aptamers were subcloned into a bacterial expression vector ($pET30a^+$). Following protein expression, protein purification, and refolding, the peptide aptamers were used for *in vitro* binding assays. Whole cell extracts of RPMI 8226 cells were incubated with recombinant peptide aptamers, which were incubated with anti-Stat3 antibodies and Sepharose A beads. Bound protein complexes were eluted and the samples were analyzed by SDS-PAGE and Western blotting. Peptide aptamer molecules present in a complex with Stat3 were visualized with an antibody specific for the scaffold protein Trx. Peptide aptamers selected for interaction with the Stat3-DD also formed complexes with Stat3 *in vitro* (Fig. 1C). Only weak interactions of peptide aptamer DBD-1 with Stat3 were detectable (Fig. 1C). The Trx wild-type protein without peptide insert (Trx) did not interact with Stat3 and served as a negative control (Fig. 1C). These results indicate that the recombinant forms of the selected peptide aptamers are able to interact with cellular Stat3 *in vitro*.

Peptide Aptamers Interfere With Intracellular Stat3 Signaling

The mere binding ability of the peptide aptamers to Stat3 does not necessarily imply functional interference with the Stat3 signaling pathway. To test the ability of the selected peptide aptamers to interfere with Stat3 signaling functions *in vivo*, we subcloned the peptide aptamer sequences into an eukaryotic expression vector (pRc/CMV-VP22-Trx) and introduced these

constructs into Herc cells. Herc cells are NIH3T3 fibroblasts stably transfected with the human *EGFR* gene (49). On stimulation with EGF, Stat3 is activated through phosphorylation on tyrosine 705, most likely due to the recruitment of the c-Src kinase to the EGFR (50).

We tested whether the selected peptide aptamers interfere with the transactivation potential of Stat3 in transiently transfected Herc cells. Increasing amounts of plasmids encoding peptide aptamers DD-1, DD-2, or DBD-1 were cotransfected with a Stat3-dependent luciferase reporter gene (*αMG-luc*). Luciferase activity was measured in starved cells (medium without FCS) and in cells induced overnight with EGF (50 ng/ml) and the ratio was calculated. The presence of the peptide aptamers DD-1, DD-2, and DBD-1 caused a dose-dependent decrease in Stat3-dependent luciferase reporter activity when compared with cells transfected with the Trx encoding construct, without a peptide aptamer insert, or control cells (Fig. 2A).

The growth of Herc cells is not dependent on constitutive Stat3 signaling. For this reason, these cells were used to derive Herc cells stably expressing the peptide aptamers. Cells were transfected and grown for 2 weeks in selective conditions (1 mg/ml G418) and stably transfected clones were obtained. The expression level of peptide aptamers in single clones was analyzed in Western blots with an anti-Trx antibody (Sigma Chemical Co., Taufkirchen, Germany; Fig. 2B, *bottom*). These stably transfected cell clones were used to study the peptide aptamer-mediated inhibition of Stat3 activation. The Trx wild-type protein showed the highest expression levels followed by clone DD-2-C1. Three clones from peptide aptamer DD-1 showed different expression levels of the peptide aptamers (DD-1-C1, DD-1-C4, and D-1-C10). The cell clones expressing DD-1-C1 or DBD-1-C1 showed similar peptide aptamer expression levels. DNA binding activity and the tyrosine phosphorylation of Stat3 upon EGF stimulation of the cells were analyzed. Stat3 upon DNA binding activity was determined in whole cell extracts of stably transfected Herc cells by electrophoretic mobility shift assays (EMSA) using the radiolabeled high-affinity mutant of the sis-inducible element (51). All three peptide aptamers, DD-1, DD-2, and DBD-1 (Fig. 2B, *lanes 4–8*), caused a strong reduction of EGF-induced Stat3 DNA binding activity when compared with samples obtained from Herc cells transfected with the Trx encoding construct (Fig. 2B, *lanes 1–3*).

We measured the induction of Stat3 tyrosine 705 phosphorylation following EGF stimulation of Herc cells stably transfected with constructs encoding the peptide aptamers DD-1, DD-2, or DBD-1 and compared them to untransfected Herc control cells (Fig. 3A). For this purpose, a specific antibody exclusively recognizing the phosphotyrosine 705 of Stat3 was used. The expression of peptide aptamer DD-1 or DD-2 reduced EGF-induced tyrosine phosphorylation of Stat3 in all four cell clones examined (Fig. 3A, *lanes 4–7*). The peptide aptamer construct encoding DBD-1 did not reduce the EGF-induced Stat3 phosphorylation (Fig. 3A, *lane 8*).

We investigated if the presence of the peptide aptamers would effect the phosphorylation status of the EGFR and other established signal events downstream of the EGFR (*e.g.*, MAPK activation; Ref. 52). To address the activation status of the EGFR, lysates of stable transfected Herc cells were prepared and the EGFR was immunoprecipitated with an EGFR-specific antibody. The tyrosine phosphorylation status of the receptor was monitored in Western blot analysis using a phosphotyrosine-specific antibody. A strong increase in tyrosine phosphorylation can be detected in wild-type Herc cells following EGF treatment compared with unstimulated cells (Fig. 3B, *lanes 1 and 2*). No changes on the activation status of the EGFR was observed in Herc cells stable expressing the wild-type Trx protein and in cells stably transfected with

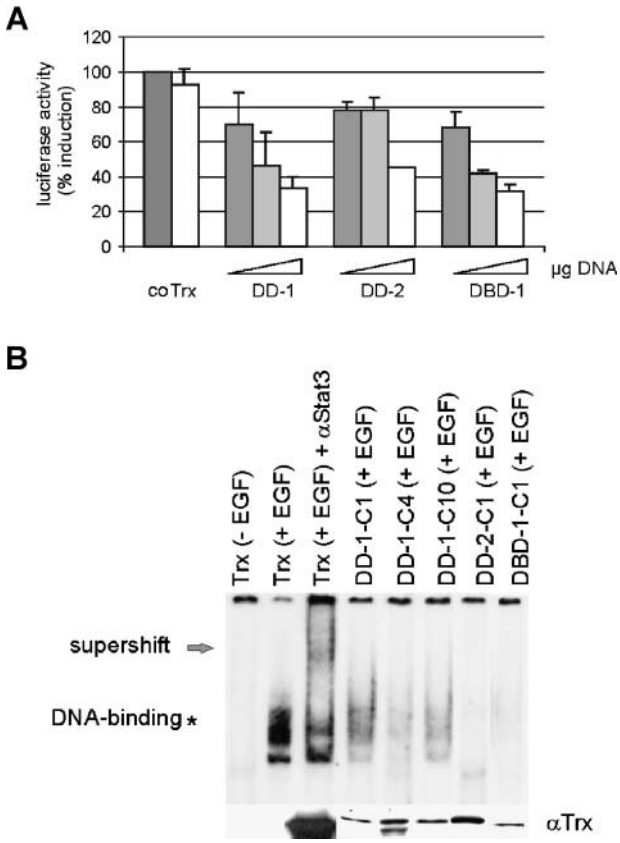

FIGURE 2. Peptide aptamers inhibit Stat3 signaling in Herc cells. **A.** Peptide aptamers inhibit Stat3 transactivation in transiently transfected Herc cells. Herc cells were transiently transfected with increasing amounts of pRc/CMV-VP22 peptide aptamer vectors (0.5, 1, or 1.5 μg or 1.5 μg pRc/CMV-VP22-Trx), Stat3 luciferase reporter construct (500 ng), and β-galactosidase expression plasmid (30 ng). Twenty-four hours after transfection, cells were starved in serum-free medium for 10 h followed by EGF treatment (50 ng/ml) overnight. Luciferase activity was measured and normalized for transfection efficiency using β-galactosidase activity as an internal control. Fold induction was calculated as the ratio of light units from stimulated to unstimulated luciferase activity. Fold induction of wild-type cells was set to 100%. Peptide aptamers significantly decreased Stat3 transactivation compared with control and Trx-transfected cells ($P \leq 0.05$). *Columns,* means of three independent experiments; *bars,* SD. **B.** DNA binding activity of Stat3 is reduced in Herc cells stably transfected with peptide aptamers. Stat3 DNA binding activity was determined *via* EMSA using whole cell extracts (4 μg) and a ^{32}P-labeled oligonucleotide probe containing a consensus binding motif for Stat3 (high-affinity mutant of the sis-inducible element). For supershift analysis, whole cell extracts were preincubated with specific antibody for Stat3 (Santa Cruz Biotechnology). *Bottom,* expression levels of the peptide aptamers. C1, C4, and C10 are single clones of transfected cells. *Arrow,* supershift; *asterisk,* DNA binding.

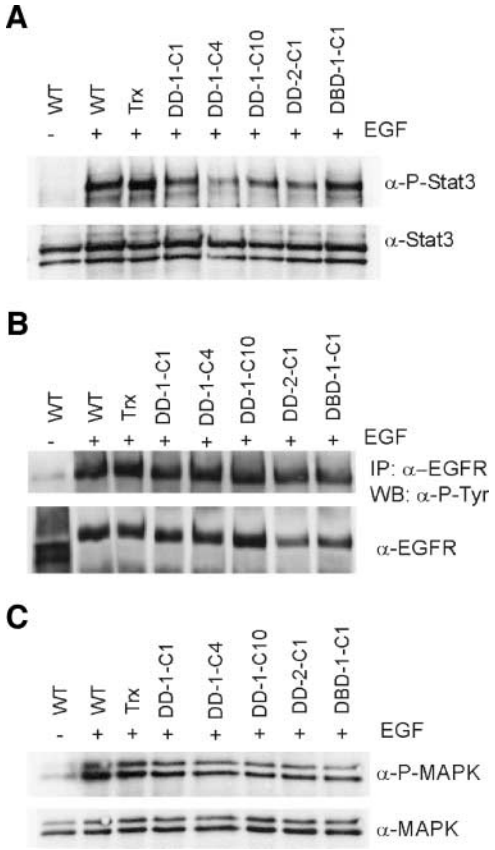

FIGURE 3. DD peptide aptamers specifically interfere with Stat3 phosphorylation. **A.** EGF-induced phosphorylation of Stat3 is reduced in Herc cells in the presence of DD peptide aptamers. Stably transfected Herc cells were starved overnight and induced with EGF (50 ng/ml) for 20 min and harvested. Cell lysates (50 μg) were subjected to Western blot analysis using a phospho-Stat3-specific antibody. After stripping, the membrane was reprobed with a total Stat3-specific antibody to ensure equal loading. **B** and **C.** Activation of EGFR and the downstream target MAPK p42/p44 is not affected in the presence of peptide aptamers. Stably transfected Herc cells were starved overnight and induced with EGF (50 ng/ml) for 20 min and harvested. **B.** EGFR was precipitated with an EGFR-specific antibody. Complexes were subjected to Western blotting, where the phosphorylation status of the receptor was detected using an anti-phosphotyrosine-specific antibody. Reprobing the blot with an anti-EGFR-specific antibody revealed equal protein amounts loaded on the gel. **C.** Total lysates were subjected to Western blot analysis using specific anti-phospho-MAPK p42/p44 antibodies. To monitor equal loading, the membrane was stripped and reprobed with an antibody recognizing total p42/p44 MAPK.

constructs encoding the peptide aptamers DD-1, DD-2, or DBD-1 (Fig. 3B, *lanes 3–8*). We also measured the activation of the MAPK p42/p44 following EGF treatment of Herc cells. Induction of phosphorylation (PT202/PY203) was detectable in wild-type Herc cells treated with EGF and in cells stably transfected with constructs coding for wild-type Trx protein or peptide aptamers DD-1, DD-2, or DBD-1 (Fig. 3C).

Our results show that the selected peptide aptamers can interfere with the Stat3 signaling pathway by reducing tyrosine phosphorylation (DD-1 and DD-2) or by preventing DNA binding (DD-1, DD-2, and DBD-1) and thus cause a significant reduction of Stat3-mediated transactivation.

Peptide Aptamer DBD-1 Inhibits Stat3 Signaling in Murine Melanoma Cells

We investigated the potential of selected peptide aptamers to interfere with Stat3 signaling in tumor cell lines in which Stat3 is constitutively activated [*e.g.*, murine melanoma B16 cells (17) and human myeloma U266 cells (16)]. For both cell types, their survival is dependent on constitutive Stat3 signaling. Recent studies showed that blocking of Stat3 signaling in B16 and U266 cells leads to cell death (17).

B16 cells were cotransfected with constructs encoding peptide aptamers and a Stat3-dependent luciferase reporter gene. Thirty-six hours later, luciferase activities were measured in cell extracts. The expression of a construct encoding DBD-1 caused a strong reduction of luciferase activity when compared with control cells or cells transfected with the Trx expression vector (Fig. 4A). No significant effect was observed with peptide aptamer DD-1 or peptide aptamer DD-2 (Fig. 4A).

Constitutively activated Stat3 seems to be essential for growth and survival of the B16 cells (17, 21). We examined the effect of peptide aptamers on the viability of B16 cells.

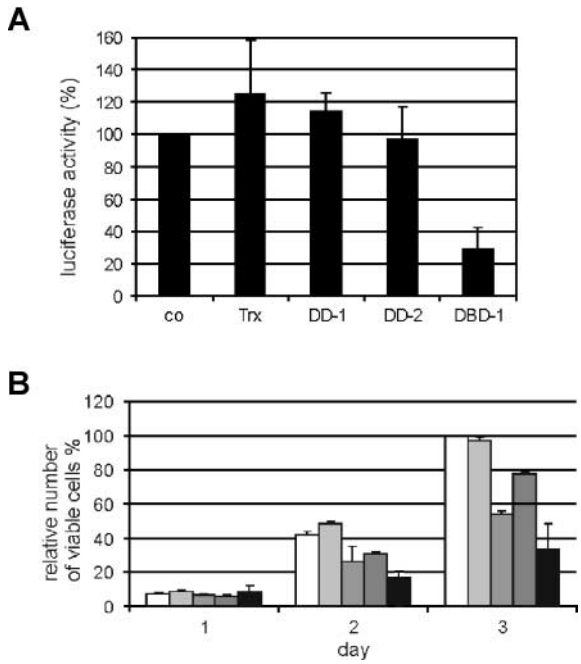

FIGURE 4. Peptide aptamer DBD-1 reduces Stat3-mediated transcriptional activity and decreases viability in B16 cells. **A.** B16 cells were transiently transfected with indicated pRc/CMV-VP22 peptide aptamer vectors (1.5 μg), a Stat3 luciferase reporter construct (500 ng), and a β-galactosidase expression plasmid (30 ng). Thirty-six hours after transfection, luciferase activity was measured and normalized for transfection efficiency using β-galactosidase activity as an internal control. Luciferase activity of wild-type cells was designated to 100%. Peptide aptamer DBD-1 significantly inhibits Stat3 activity ($P \leq 0.05$). *Columns,* means of three independent experiments; *bars,* SD. **B.** B16 cells were transiently transfected with indicated pRc/CMV-VP22 peptide aptamer vectors (2 μg) and seeded in triplicates in 96-well plates. Every 24 h, relative number of viable cells was assessed using the XTT-based proliferation kit (Roche Molecular Biochemicals). Peptide aptamer DBD-1 significantly reduced relative numbers of viable cells ($P \leq 0.05$). *Columns,* means of three independent experiments; *bars,* SD. □, Control; ▨, Trx; ▩, DD-1; ▩, DD-2; ■, DBD-1.

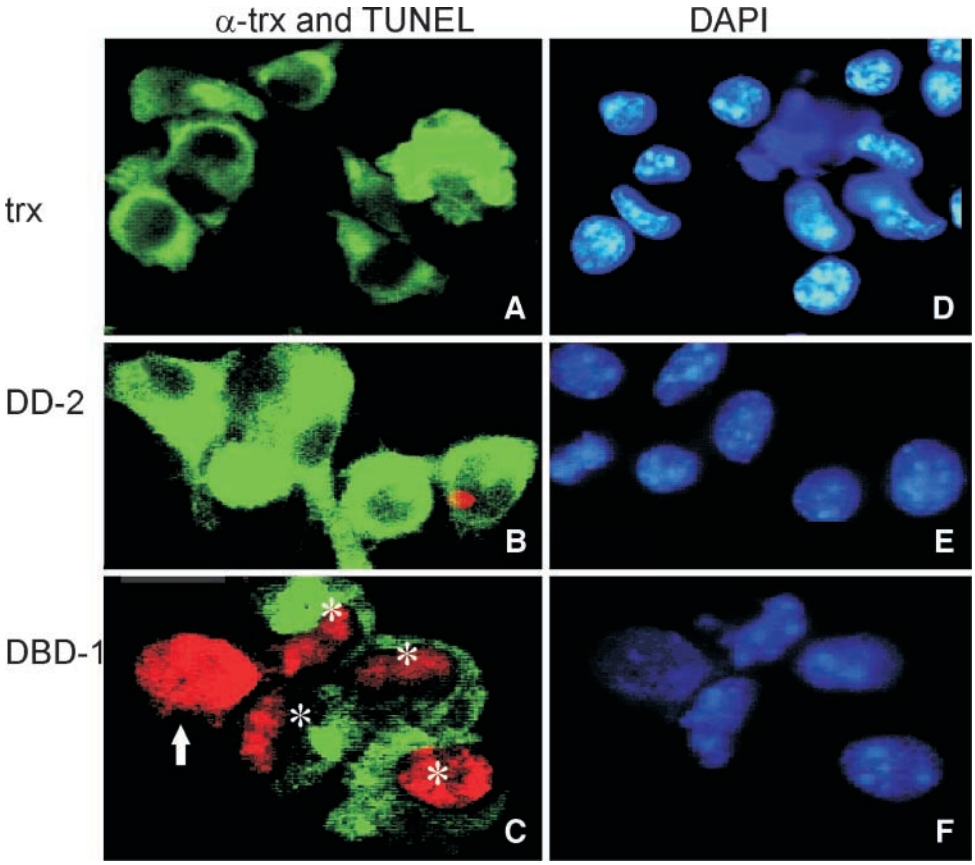

FIGURE 5. DBD-1 induces apoptosis in B16 cells. Murine melanoma cells (B16) were transiently transfected with indicated pRc/CMV-VP22 peptide aptamer vectors (2 μg). Forty-eight hours after transfection, cells were stained for DNA fragmentation (TUNEL; *red*) followed by indirect immunostaining for peptide aptamer expression (anti-Trx antibody; *green*). Nuclei were stained with 4′,6-diamino-2-phenylindole (*blue*). *Asterisks,* TUNEL-positive and transfected B16 cells; *arrow,* TUNEL-positive but untransfected cell.

Cell proliferation and viability were measured in a 2,3-bis [2-methoxy-4-nitro-5-sulfophenyl]-2H-tetrazolium-5-carboxanilide inner salt (XTT)-based test. Following transfection with the peptide aptamer encoding constructs, B16 cells were seeded into a 96-well plate. In 24 h intervals, the relative number of viable cells was determined with XTT. Cells Transfection with peptide aptamers DBD-1, DD-1, and DD-2 caused a significant decrease in B16 cell viability when compared with Trx-transfected cells or control B16 cells (Fig. 4B). Comparison of the three peptide aptamer indicates that peptide aptamer DBD-1 significantly inhibits with the highest efficiency. Induction of apoptosis was visualized in a terminal deoxynucleotidyl transferase-mediated nick end labeling (TUNEL) assay. Following transient transfection of B16 cells, the expression of the peptide aptamer construct was monitored by indirect immunofluorescence with an antibody recognizing Trx (Fig. 5, *green*). The induction of apoptosis was monitored by TUNEL staining (Fig. 5, *red*). B16 cells expressing peptide aptamer DBD-1 stained TUNEL positive (Fig. 5C, *asterisks*). Quantification of apoptotic cells revealed that transfection of peptide aptamer DBD-1 resulted in ~50% of all cells undergoing apoptosis (Table 1). In contrast, only about 2% of cells expressing Trx or peptide aptamers DD-1 or DD-2 showed DNA fragmentation (Table 1).

Our TUNEL assays of B16 cells transfected with the DBD-1 peptide aptamer indicate that not only DBD-1 expressing cells undergo apoptosis but also adjacent untransfected cells are affected (Fig. 5C, *arrow*). We therefore compared in a more detailed analysis of our TUNEL assays the number of peptide aptamer expressing cells and TUNEL-positive cells (Trx+/TUNEL+) with nonexpressing but TUNEL-positive cells (Trx−/TUNEL+). Following transfection of Trx, DD-1 or DD-2 constructs, apoptosis was mostly detectable in cells expressing the peptide aptamers (Trx+/TUNEL+) and <0.5% of untransfected cells (Trx−/TUNEL+) became TUNEL positive (Table 1). In contrast, transfection of peptide aptamer DBD-1 resulted in 11% of Trx−/TUNEL+ cells, indicating a bystander effect

TABLE 1. Quantification of TUNEL-Positive B16 cells Following Transfection of Peptide Aptamers

Peptide Aptamer	TUNEL+ (% of All Cells)	Trx+/TUNEL+ (% of All Cells)	Trx−/TUNEL+ (% of All Cells)
Co	2.0	2.0	0.0
Trx	2.9	2.7	0.2
DD-1	2.3	2.0	0.3
DD-2	2.1	1.9	0.2
DBD	51.1	40.0	11.1

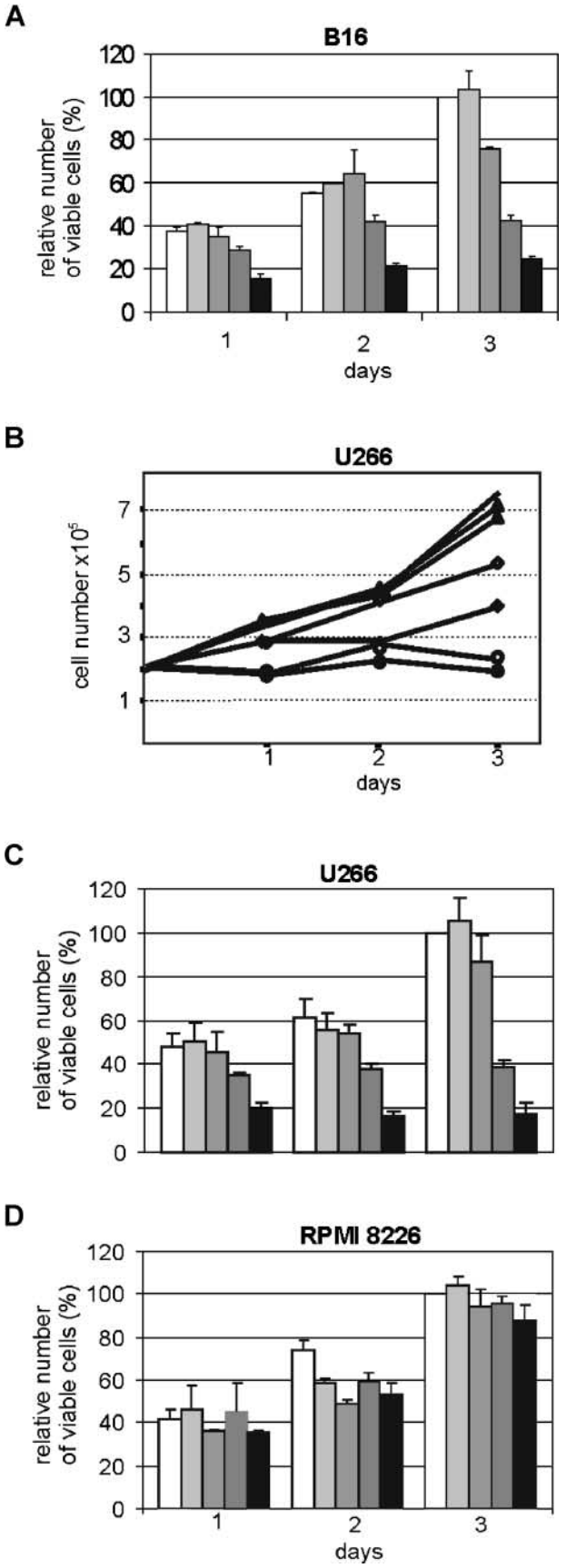

induced by peptide aptamer DBD-1 (Table 1). These results show that peptide aptamer DBD-1-mediated inhibition of Stat3 signaling can trigger apoptosis in murine melanoma cells. Because the peptide aptamers against the Stat3-DD seemed less effective than peptide aptamer DBD-1 in their biological effects, peptide aptamer DBD-1 was preferentially used for further analyses.

Recombinant Cell-Penetrating Form of Peptide Aptamer DBD-1 Inhibits Growth of Tumor Cells and Induces Apoptosis Human Myeloma Cells

We analyzed the potency of cell-penetrating peptide aptamer DBD-1 with respect to Stat3 inhibition and its effects on growth and survival of tumor cells. A fusion protein comprising an optimized PTD consisting of nine L-arginine residues (28) and the peptide aptamer sequence DBD-1 were constructed, expressed in bacteria, and purified. B16 cells were treated every 12 h with 180 or 360 nM of peptide aptamer DBD-1-9R or Trx-9R and relative cell numbers were determined with XTT. Transduction of peptide aptamer DBD-1-9R caused a dose-dependent decrease in relative B16 cell viability when compared with cells treated with Trx-9R or control B16 cells (Fig. 6A).

The growth inhibitory effect of DBD-1-9R was confirmed with a second cell line exhibiting constitutive Stat3 activation. U266 cells were transduced in 12 h intervals with the PTD peptide aptamer protein. Increasing amounts of peptide aptamer DBD-1-9R or Trx-9R were added and the cell numbers were determined in 24 h intervals. Addition of 180–450 nM of purified recombinant peptide aptamer DBD-1-9R inhibited proliferation in a dose-dependent manner. A 50% growth inhibition compared with control cells was found with 270 nM

FIGURE 6. Dose-dependent growth inhibition of tumor cells transduced with peptide aptamer DBD-1-9R. **A.** B16 cells (10^3 cells/well) were seeded and transduced every 12 h with indicated concentration of peptide aptamer DBD-1-9R or Trx-9R. As control, cells were treated with dialysis buffer. Every 24 h, relative number of viable cells was assessed in triplicates using the XTT-based proliferation kit (Roche Molecular Biochemicals) in 96-well plates. Control-treated cells were assigned to 100%. DBD-1-9R significantly reduced relative numbers of viable cells compared with control and Trx-9R-treated cells ($P \leq 0.05$). *Columns,* means of three independent experiments; *bars,* SD. **B** and **C.** Dose-dependent growth inhibition in human myeloma cells transduced with DBD peptide aptamer. U266 cells (2×10^5 cells/ml) were seeded and transduced every 12 h with indicated concentration of peptide aptamer DBD-1-9R or Trx-9R. As control, cells were treated with dialysis buffer. □, Control; ▫, Trx (180 nM); ▪, Trx (360 nM); ▪, DBD-1 (180 nM); ■, DBD-1 (360 nM). **B.** Cell numbers were determined in 24 h intervals. —, Control; —△—, Trx; —▲—, DBD-1 (90 nM); —◇—, DBD-1 (180 nM); —◆—, DBD-1 (270 nM); —○—, DBD-1 (360 nM); —●—, DBD-1 (450 nM). **C.** Every 24 h, relative number of viable cells was assessed using the XTT-based proliferation kit (Roche Molecular Biochemicals). Control-treated cells were assigned to 100%. DBD-1-9R significantly reduced relative numbers of viable cells compared with control and Trx-9R-treated cells ($P \leq 0.05$). □, Control; ▫, Trx (180 nM); ▪, Trx (360 nM); ▪, DBD-1 (180 nM); ■, DBD-1 (360 nM). *Columns,* means of three independent experiments; *bars,* SD. **D.** RPMI 8226 cells (2×10^5 cells/ml) were seeded and transduced every 12 h with indicated concentration of peptide aptamer DBD-1-9R or Trx-9R. As control, cells were treated with dialysis buffer. Every 24 h, relative number of viable cells was assessed using the XTT-based proliferation kit (Roche Molecular Biochemicals). Control-treated cells were assigned to 100%. DBD-1-9R slightly reduces relative number of viable cells compared with Trx-9R and control treated cells. □, Control; ▫, Trx (180 nM); ▪, Trx (360 nM); ▪, DBD-1 (180 nM); ■, DBD-1 (360 nM).

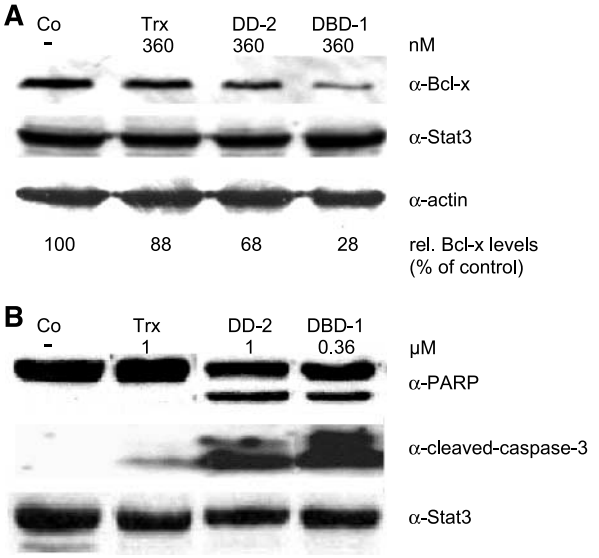

FIGURE 7. Peptide aptamer DBD-1 and DD-2 induce proapoptotic markers in U266 cells. **A.** Bcl-x_L expression is down-regulated in cells transduced with peptide aptamers. U266 cells were transduced with indicated peptide aptamers (360 nM) every 12 h for 2.5 days. Western blot analyses were performed using whole cell extracts (80 μg) and probed with Bcl-x_L, Stat3, and actin antibodies. Buffer-treated and Trx-9R-treated cells served as negative controls. Quantification of the Bcl-x_L levels was normalized to the actin levels with the TINA software. **B.** Cleavage of caspase-3 and PARP in DD-2- and DBD-1-transduced cells. Cells were treated with DBD-1-9R (360 nM), DD-2-9R (1 μM), or Trx-9R (1 μM) to study caspase-3 and PARP cleavage. RIPA extracts (100 μg) were subjected to immunoblot analysis using a caspase-3 antibody, which recognizes the cleaved fragments (17 and 19 kDa) and an anti-PARP antibody that recognizes full-length PARP and the cleaved 89 kDa fragment. Membrane was reprobed with anti-Stat3 antibodies to ensure equal loading.

DBD-1-9R (Fig. 6B). U266 cells transduced with very high concentrations of Trx-9R showed only a slight decrease in growth compared with control cells (Fig. 6B). Transduction with lower concentrations of Trx-9R had no effect (data not shown). In addition to cell numbers, we performed XTT tests. U266 cells were treated every 12 h with 180 or 360 nM of peptide aptamer DBD-1-9R or Trx-9R and relative number of viable cells was determined with XTT. Again, peptide aptamer DBD-1-9R caused a dose-dependent decrease in U266 cell viability when compared with Trx-9R-treated or control U266 cells (Fig. 6C).

To test the specificity of peptide aptamer DBD-1 with respect to its ability to induce apoptosis, we have compared the effects of this aptamer on Stat3-dependent and Stat3-independent cell lines. For this purpose, transduction experiments were performed with the human myeloma cell line RPMI 8266 (Fig. 6D). It has been shown previously that the growth and survival of these cells is not dependent on Stat3 activity (16). RPMI 8226 cells were transduced with peptide aptamer DBD-1-9R, Trx-9R, or buffer and relative number of viable cell was measured in XTT tests. In contrast to the Stat3-dependent U266 cells, peptide aptamer DBD-1-9R only slightly reduces the relative number of viable RPMI 8226 cells at very high concentrations when compared with control and Trx-9R-treated cells.

We analyzed the effects of the transduced PTD peptide aptamer DBD-1 on the induction of cellular apoptosis on molecular levels. The connection between Stat3 activation and inhibition of apoptosis is possibly due to the fact that transcription of the antiapoptotic protein Bcl-x_L is induced by Stat3 in U266 cells. Inhibition of Bcl-x_L expression can result in the induction of apoptosis (16). We analyzed the influence of

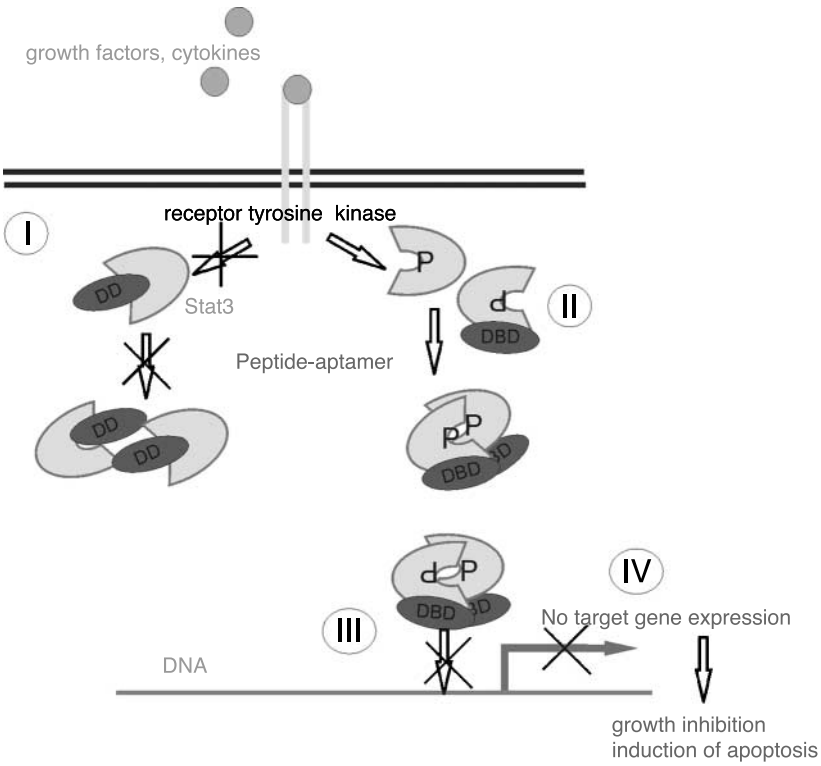

FIGURE 8. Model for the inhibition of Stat3 signaling by peptide aptamers. Peptide aptamers selected for interaction with the Stat3-DD associate with monomeric Stat molecules form a complex and as a consequence, prevent phosphorylation of Stat3 molecules (*I*). Peptide aptamer DBD-1, which was selected for interaction with Stat3-DBD, does not interfere with the phosphorylation of Stat3 (*II*) but block the binding of Stat3 molecules to the DNA (*III*). As a result of inhibiting either the phosphorylation or the DNA binding of Stat3 molecules, Stat3 signaling is blocked and the transcription of target genes is reduced (*IV*). As a result of the inhibition of Stat3 activation, phenotypical changes including growth inhibition and/or induction of apoptosis occur in Stat3-dependent tumor cells.

transduced peptide aptamers with Stat3-dependent expression of Bcl-x_L. The cells were treated with 360 nM of peptide aptamers DBD-1-9R, DD-2-9R, or Trx-9R and Bcl-x_L protein levels were detected by Western blotting. A strong down-regulation of Bcl-x_L levels was observed in U266 transduced with peptide aptamer DBD-1-9R (Fig. 7A, *lane 4*). Only a weak decrease of Bcl-x_L expression was detectable in DD-2-9R-treated cells (Fig. 7A, *lane 3*). No changes in the Bcl-x_L levels occurred in Trx-9R-treated cells when compared with control cells (Fig. 7A, *lanes 1 and 2*). A quantitative evaluation of the Bcl-x_L expression levels is shown in the lower panel.

Reduced levels of the Bcl-2 family member Bcl-x_L lead to changes in the ratio of Bcl-x_L/proapoptotic Bcl-2 family members (*e.g.*, Bad and Bax) and induce cytochrome *c* release (53). This leads to the activation of caspases (*e.g.*, the effector caspase-3), which then cleave several substrates [*e.g.*, poly-ADP-ribosyl polymerase (PARP; Ref. 54)]. PARP degradation and detection of its cleavage products indicate apoptosis (55). The connection between the reduced expression levels of the antiapoptotic protein Bcl-x_L in our transduction experiments (Fig. 7A) and the induction of apoptosis was further assayed by measurement of cleaved caspase-3 and PARP in immunoblots. Proteolytic caspase-3 and PARP fragments were detected in U266 cells transduced with 360 nM peptide aptamer DBD-1 (Fig. 7B). Treatment of the cells with peptide aptamer DD-2 (1 μM) also induced caspase-3 and PARP cleavage. Neither caspase-3 cleavage nor PARP fragments were observed in control cells or cells transduced with 1 μM Trx-9R (Fig. 7C). These results indicate that exogenously introduced peptide aptamer DBD-1-9R protein can cause a decrease in the intracellular levels of the Stat3 target gene *Bcl-x_L* in human myeloma cells and thereby induce apoptosis.

Based on these results, we propose a model for the interaction of peptide aptamers with Stat3 molecules and their inhibition of Stat3 signaling functions (Fig. 8). Peptide aptamers selected for interaction with the Stat3-DD associate with monomeric Stat molecules and prevent tyrosine 705 phosphorylation (I). Peptide aptamer DBD-1 selected for interaction with the Stat3-DBD does not interfere with the phosphorylation of Stat3 (II) but blocks the binding of Stat3 to DNA (III). Inhibition of either the phosphorylation or the DNA binding function of Stat3 reduces the transcription of target genes (IV).

Discussion

Stat3 signaling in various tumor cells is essential for their growth and survival. The activation of Stat3 requires several well-defined events—phosphorylation, dimerization, DNA binding, and association with accessory proteins. Most of these functions have been assigned to distinct functional domains within the molecule and it is tempting to think about targeted interference strategies. Especially, the Stat3-DD and the Stat3-DBD, responsible for crucial molecular interactions, could possibly be exploited.

To interfere with these functions of the Stat3 molecule, compounds are required which prevent specific protein-protein or protein-DNA interactions. Studies with model compounds [*e.g.*, the p53-Mdm2 system (56)] have shown that specific peptides constituting part of a known interface in protein-protein interactions can be used for this purpose. Tyrosine-phosphorylated peptides have also been used to interfere with Stat3 dimerization or receptor recruitment in cultured cells (14). In our study, we have used an approach that does not *a priori* require exact information about interaction interfaces. It is based on a high complexity peptide aptamer library from which we isolated peptides capable of intracellular binding to crucial domains of Stat3. Interference with the biological function of Stat3 was then established in a second step. Peptide sequences, which bind to the Stat3-DD, containing tyrosine 705 or Stat3-DBD, led to several candidates to be tested.

Three clones obtained using the Stat3-DD bait construct contained 42 amino acid inserts. We assume that two copies of the random synthetic peptide aptamer nucleotide sequences were integrated into the expression vector during the cloning of the library (see "Results"). The sequence within Stat3, which mediates homodimerization, involves the region around the phosphotyrosine 705 of one and the SH2 domain (amino acids 689–701) of the second interaction partner (51). This SH2 domain motif could conceivably interact with the region around the phosphotyrosine 705 used as bait in our screen, but no sequence similarity was detected in the DD-1 to DD-3 peptide aptamers (Fig. 1, A and B). We also could not detect homologies to known Stat3-inhibitors [*e.g.*, consensus sequences of phosphopeptide binding motifs that recognize the Stat3 SH2 domains like PY*LKTK, Y*XXI, and Y*XXM, the asterisks indicating phosphorylated tyrosine residues (14, 15)]. The region used in the bait construct in yeast cells comprised the SH2 domain and additional flanking sequences. The exact binding epitope is therefore not precisely defined. Peptide aptamers interacting with this epitope, however, prevent phosphorylation and dimerization of Stat3.

The second bait construct (Stat3-DBD) contained part of the Stat3-DBD (amino acid positions 322–483). This region of the Stat3 molecule is responsible for the interaction with specific DNA sequences in the promoter region of target genes (48). Using this bait construct, we were able to isolate one clone containing a 20 amino acid insert (DBD-1; see "Results"). In contrast to the *in vivo* experiments, DBD-1 exhibits only weak *in vitro* binding to Stat3 (Fig. 1, B and C). This might be a result of the *in vitro* renaturation conditions of the recombinant protein. It is also possible that *in vivo* screening procedure detects interactions that are not readily detectable *in vitro* (36).

Molecular Interference of Peptide Aptamers With the Stat3 Signaling Pathway

The interference of isolated peptide aptamers with Stat3 signaling was analyzed *in vivo* in Herc cells. In the presence of Stat3-DD peptide aptamers, the transactivation activity and the DNA binding activity of Stat3 were inhibited as shown in reporter gene assays and EMSAs (Fig. 2, A and B). Western blot analysis with a phosphotyrosine-specific Stat3 antibody showed that the molecular mechanism underlying this inhibition was a reduced Stat3 phosphorylation on tyrosine 705. These data clearly show that the isolated peptide aptamers

interfere with Stat3 signaling and suppress Stat3 function. Similar effects have been obtained previously by using peptidomimetics, which also interfere with Stat3 phosphorylation (14, 15, 20).

The DBD peptide aptamer inhibits DNA binding as well as the transactivation activity of Stat3. However, in contrast to the peptide aptamers DD-1 and DD-2, the DBD peptide aptamer does not interfere with the phosphorylation of Stat3 (Fig. 3A). These results suggest that peptide aptamers can be used for inhibiting individual steps in the activation scenario of Stat3. Depending on the binding site of the peptide aptamer, individual aspects of activation can be disturbed without affecting neighboring functional domains. This might become an advantage when compared with gene targeting approaches. Small interference RNA-based gene silencing results in an elimination of mRNA and eventually of the entire protein. Individual functional capabilities present in a single polypeptide cannot be addressed independently. Further refinement of the peptide aptamer technology might allow that peptide aptamers can be used to define functional domains of proteins and identify their downstream targets.

Stat3 Peptide Aptamers As Therapeutic Agents in Cancer Treatment

Tumor cells are characterized by deregulated proliferation and resistance to proapoptotic stimuli (1). The most commonly used chemotherapeutics inhibit tumor growth and eliminate tumors by inducing apoptosis (57). Tumor cells in turn can evade the action of chemotherapeutic drugs through the overexpression of antiapoptotic proteins. Down-regulation or inhibition of these antiapoptotic proteins might result in the sensitization of tumor cells to chemotherapeutic drugs and improve therapeutic success. Stat3 is an important target in this respect; it is involved in the regulation of genes that promote cell cycle progression and genes that protect against programmed cell death either by activation of gene transcription (16, 23) or by acting as a transcriptional repressor (21, 22).

In the present study, tumor cell lines in which Stat3 is constitutively activated (B16 or U266 cells) were used to examine the effects of the isolated peptide aptamers on cell growth and survival. Peptide aptamers DD-1 and DD-2 did not influence Stat3 signaling in the murine B16 melanoma cell line on transfection of the encoding constructs. We suspect that the intracellular concentrations achieved on transfection might be not high enough to interfere with Stat3 signaling in B16 cells. Our transduction experiments in U266 tumor cells also indicate that much higher DD-2 peptide aptamer concentrations are required, when compared with the DBD peptide, to achieve biological effects (Fig. 7). Our results with Herc cells indicate that the DD peptide aptamers are able to target monomeric Stat3 and thereby inhibit Stat3 phosphorylation and its transactivation function (Figs. 2, A and B, and 3A). However, to interfere with already existing Stat3 dimers, higher aptamer concentrations may be required (Fig. 7).

In contrast to the DD peptide aptamers, DBD-1 can cause phenotypic changes in tumor cells, inhibit proliferation, and induce apoptosis. Transient transfection of a peptide aptamer DBD-1 encoding construct into B16 melanoma cells reduced the transcriptional activity of Stat3 and cell viability and induced apoptosis in ~50% of the cells. This represents an increase in apoptosis of >25-fold over control cells and indicates that peptide aptamer DBD-1 has a strong potency to kill B16 tumor cells (Fig. 5; Table 1). Other inhibitors have been used before in similar experiments. The treatment of cell lines expressing constitutively activated Stat3 with the newly identified Stat3 small molecule inhibitor JSI-124 resulted in an increase of apoptosis of 11.1–17.6% *in vitro* and inhibited tumor cell growth and survival of mice *in vivo* (20). Similar observations have been made on transfection of a dominant-negative Stat3 construct into B16 tumors. It reduces tumor growth and induces apoptosis *in vivo* (17, 21).

Our TUNEL assays performed with B16 melanoma cells transfected with peptide aptamer DBD-1 revealed induction of apoptosis not only in cells expressing the peptide aptamer DBD-1 but also in adjacent untransfected cells. This bystander effect has also been observed after transfection of B16 melanoma cells with a dominant-negative variant of Stat3 (17). A recent study suggests that the bystander effect is mediated by the secretion of the proapoptotic effector TRAIL from Stat3-deprived B16 cells (21). This observation supports the notion that TRAIL is a negatively regulated target gene of Stat3. In contrast to most nontransformed cells, which are refractory to TRAIL, cancer cells are often sensitive to TRAIL-induced apoptosis *in vitro* and *in vivo* (58, 59). For this reason, TRAIL is being used for therapeutic purposes and treatment of melanomas with a TRAIL-based therapy has yielded promising results (58). We will investigate if inhibition of Stat3 by the peptide aptamer DBD-1 might increase the expression and secretion of TRAIL and if this mechanism plays a role in the induction of apoptosis.

A second proapoptotic event caused by DBD-1 application is the down-regulation of the antiapoptotic protein Bcl-x_L in human myeloma cells (Fig. 7A). Overexpression of Bcl-x_L has been observed in tumor cells and contributes to neoplastic cell expansion by suppressing programmed cell death and extending tumor cell life span (60). In addition, several studies indicate a correlation between Bcl-2 or Bcl-x_L overexpression with unfavorable prognosis and decreased response to chemotherapy (61, 62). For this reason, the interference with Bcl-x_L function is an attractive target for the development of new anticancer drugs. Antisense approaches as well as small molecule inhibitors have already been tested for the inhibition of Bcl-x_L function and the induction of apoptosis in target cells (63–67). Our studies show that interfering with Stat3 signaling in human myeloma cells by transduction of peptide aptamers causes the down-regulation of Bcl-x_L expression. In line with a previous study, reduced Bcl-x_L levels result in the induction of apoptosis (Fig. 7; Ref. 16).

Selected peptide aptamers with a predetermined binding ability to specific domains of central signaling components should become useful tools for the study of gene function and possibly for therapeutic purposes. The development of peptide aptamers as therapeutic agents is still in its early stages. However, the fusion of peptide aptamers with a PTD, the possibility to produce such a recombinant protein in bacteria and deliver it into cells from the exterior, makes peptide aptamers assume drug-like properties. Future studies will be focused on the identification of the most suitable target structures, the efficiency of delivery of the peptide aptamers,

and their *in vivo* applicability. For example, the introduction of non-natural amino acids could enhance binding ability and increase intracellular stability (56, 68). Ongoing studies will reveal if our peptide aptamers fused to the nine arginine PTD sequence can be delivered to all tissues and even cross the blood-brain barrier as has been described for other fusion constructs (32). Such fusion proteins could be useful also in the treatment of neurodegenerative diseases (24, 25, 35, 69). Moreover, reducing the size of the peptide aptamers fusion proteins could improve their bioavailability. This could be achieved by integrating the peptide aptamers into a minimal Trx scaffold or by adding a single cysteine residue at the COOH and NH_2 termini of the peptide. This might allow for the formation of a disulfide bond and a constrained protein conformation comparable with the one formed in the intact Trx context.

The present study shows that peptide aptamers can interfere with protein-protein and protein-DNA interactions. Peptide aptamers can be useful tools in basic research for targeting single functional domains of a given protein and the identification of downstream targets. Moreover, the present study as well as our previous data could serve as a starting point for the design of new therapeutic agents for cancer therapy.

Materials and Methods

Cell Lines and Cell Culture

Herc cells were maintained in DMEM containing 10% heat-inactivated FCS and 2 mM glutamine. Herc-Trx, Herc-DD-1, Herc-DD-2, and Herc-DBD-1 cells were generated by stable introduction of pRc/CMV-VP22-Trx-based vectors encoding for the peptide aptamer or the Trx protein without a peptide insert. Stably transfected Herc cells were maintained in DMEM containing 10% heat-inactivated FCS, 2 mM glutamine, and 1 mg/ml G418. B16 mouse melanoma cells and U266 and RPMI 8226 human myeloma cells were maintained in RPMI supplemented with 10% heat-inactivated FCS and 2 mM glutamine.

Peptide Aptamer Screening

The screening was done in the yeast strain KF-1 (MATα Trp1-901 Leu2-3112 His3-200 gal4Δ gal80Δ Lys2::GAL1-His3 GAL2-ADE2 Met2::GAL7-lacZ SPAL10-URA3; Ref. 36). As baits, part of the Stat3-DD (amino acid positions 655–755) or Stat3-DBD (amino acid positions 322–483) of murine Stat3 were fused to the GAL4-DBD into the pPC97 vector (pPC97-DD or pPC97-DBD). Screenings were done with a randomized peptide aptamer library and selection procedures were performed as described previously (36). Matings were performed with the haploid yeast strains PJ69a/α according to the manufacturer's protocol (Matchmaker3; Clontech, Heidelberg, Germany).

Bacterial Expression and Purification of PTD Peptide Aptamers

A PTD of nine arginine residues was fused to the COOH terminus of the peptide aptamers, which were inserted into the $pET30a^+$ vector (Novagen, Schwalbach, Germany). Expression of the peptide aptamer was induced with isopropyl-1-thio-β-D-galactopyranoside (0.5 mM) for 4 h at room temperature. Purification of the peptide aptamer under denaturing conditions was done as published before (70).

Immunoprecipitation

For detection the interaction of full-length Stat3 with peptide aptamers, equal amounts of RPMI 8226 cell lysates were incubated with recombinant expressed peptide aptamers for 2 h at 4°C. Afterwards, Stat3-antibody (Santa Cruz Biotechnology, Heidelberg, Germany) was added and incubated for 2 h at 4°C. Immune complexes were collected with protein A-Sepharose (Amersham Biosciences, Freiburg, Germany) and washed with PBS. Bound proteins were eluted by boiling in sample buffer and subjected to Western blotting. For detection of phosphorylated EGFR, equal amounts of lysates from stable transfected Herc cells were incubated with EGFR antibody (sc-120; Santa Cruz Biotechnology) for 2 h on ice. Immune complexes were collected with protein A-Sepharose (Amersham Biosciences) and washed twice with extraction buffer and once with TNE buffer [50 mM Tris-HCl (pH 7.5), 140 mM NaCl, 40 mM EDTA]. Bound proteins were eluted by boiling in sample buffer, subjected to SDS-PAGE, and blotted onto nitrocellulose membranes.

Western Blot Analyses

Cells were solubilized in Triton extraction buffer [50 mM Tris (pH 7.5), 5 mM EGTA, 150 mM NaCl, 1% Triton X-100, protease inhibitors] or RIPA lysis buffer [50 mM Tris (pH 7.4), 150 mM NaCl, 1% NP40, 0.5% sodium deoxycholate, 1 mM EDTA, protease inhibitors] and incubated on ice for 10 min. The lysates were clarified by centrifugation at 16,000 × *g* for 10 min. Lysates were subjected to SDS-PAGE and blotted onto nitrocellulose membranes. After blocking in 5% milk in Tris-buffered saline with Tween 20 [50 mM Tris-HCl (pH 7.5), 150 mM NaCl, 0.05% Tween 20], membranes were probed with specific antibodies and proteins were visualized with peroxidase-coupled secondary antibodies using the enhanced chemiluminescence system (Amersham Biosciences). Antibodies for EGFR (sc-03), phosphotyrosine (sc-7020), Stat3 (C20), and anti-actin were obtained from Santa Cruz Biotechnology and anti-phospho-Stat3, anti-phospho-p44/p42 MAPK, and anti-p44/p42 MAPK were from Cell Signaling-NEB (Frankfurt a. M., Germany). Anti-PARP and anti-Bcl-x_L were purchased from BD PharMingen (Heidelberg, Germany) and anti-Trx was from Sigma Chemical. The filters were stripped in SDS buffer [100 mM β-mercaptoethanol, 2% SDS, 62.5 mM Tris-HCl (pH 6.8)] for 30 min at 60°C, washed with Tris-buffered saline, blocked, and reprobed with specific antibodies.

Transfection of Eukaryotic Cells

Transfections were done with LipofectAMINE2000 (Life Technologies, Karlsruhe, Germany) according to the manufacturer's protocol. For the expression of the peptide aptamers in eukaryotic cells, the Trx cassette was subcloned into the eukaryotic expression vector pRc/CMV (Invitrogen, Karlsruhe, Germany) and fused 3′ to the herpes simplex virus *VP22* gene

(pRc/CMV-VP22-Trx). For the derivation of stable cell clones, G418 (1 mg/ml) was added to the cells 24 h after transfection with the described plasmid DNA. Single clones were picked and cultivated for 2 weeks under selective conditions. Expression levels of peptide aptamers were detected in Western blot analysis with an anti-Trx antibody (Sigma Chemical).

Luciferase Reporter Assays

Cells were transfected with α-macroglobulin promoter reporter plasmid, β-galactosidase expression plasmid, and pRc/CMV-VP22-Trx-based vectors encoding for the peptide aptamer or the Trx protein without peptide insert. Twenty-four hours after transfection, Herc cells were starved in serum-free medium, induced for 15 h with EGF (50 ng/ml), and harvested. B16 cells were harvested 36 h after transfection. Cells were lysed in Triton buffer [1% Triton X-100, 25 mM glycylglycin (pH 7.8), 15 mM $MgSO_4$, 4 mM EGTA, 1 mM DTT] for 10 min on ice. The lysates were clarified by centrifugation for 10 min at 16,000 × *g*. Lysates (10 μl) were measured using a luminometer (Berthold, Vista, CA) by injecting luciferin reagent [25 mM glycylglycin (pH 7.8), 5 mM ATP (pH 7.8), 330 mM beetle luciferin]. The samples were normalized for the β-galactosidase activity, which was measured after incubating 3 μl lysate with 33 μl reaction buffer [100 mM Na_2HPO_4, 1 mM $MgCl_2$, 1× Galacton (Tropix, Bedford, MA)] for 30 min in \the dark. The galactosidase activity was measured in a luminometer by injection of amplifier [10% Emerald (Tropix), 0.2 M NaOH].

Electrophoretic Mobility Shift Assay

Stably transfected Herc cells were starved overnight and induced with EGF for 20 min. Cells were lysed in HEPES buffer [20 mM HEPES, 0.5% sodium cholate, 0.1% SDS, 150 mM NaCl, 5 mM EDTA, 50 mM Tris (pH7.5)] by freezing and thawing thrice in liquid nitrogen. Clarified supernatant (4 μg) has been used in EMSA as described previously (71). Supershifts were performed by preincubation of the lysates for 20 min with an anti-Stat3 antibody (C20; Santa Cruz Biotechnology) at room temperature.

Proliferation and Viability Assay

Relative viable cell numbers were quantified using the XTT-based proliferation kit II according to the manufacturer's protocol, which assesses cell viability via bioreduction of a tetrazolium compound by measuring absorbance at 490 nm in a 96-well-plate reader (Roche Molecular Biochemicals, Mannheim, Germany).

TUNEL Staining and Immunofluorescence

Forty-eight hours after transfection, cells were subjected to TUNEL staining with the *in situ* cell death kit (Roche Molecular Biochemicals) according to the manufacturer's protocol followed by indirect immunostaining for peptide aptamer expression with a Trx antibody (Sigma Chemical) as described previously (72). As secondary antibody, Alexa Flour488 from Molecular Probes (Leiden, Netherlands) was used.

Acknowledgments

We thank S. Abrell for cloning the Stat3-DBD bait construct, R. Jove for providing the U266 and RPMI 8226 cells, W. Baum, C. Kunz, C. Shemanko, and I. Oehme for helpful discussions, N. Delis for technical assistance, and C. Kost, C. Gewinner, and C. Borghouts for improving the manuscript.

References

1. Hanahan D, Weinberg RA. The hallmarks of cancer. Cell, 2000;100:57–70.

2. Traxler P. Tyrosine kinases as targets in cancer therapy—successes and failures. Exp Opin Ther Targets, 2003;7:215–34.

3. Dancey J, Sausville EA. Issues and progress with protein kinase inhibitors for cancer treatment. Nat Rev Drug Discov, 2003;4:296–313.

4. Levitzki A. Tyrosine kinases as targets for cancer therapy. Eur J Cancer, 2002;38(Suppl 5):11–8.

5. Darnell JE Jr. Transcription factors as targets for cancer therapy. Nat Rev Cancer, 2002;2:740–9.

6. Levy DE, Darnell JE Jr. Stats: transcriptional control and biological impact. Nat Rev Mol Cell Biol, 2002;3:651–62.

7. Fukada T, Hibi M, Yamanaka Y, et al. Two signals are necessary for cell proliferation induced by a cytokine receptor gp130: involvement of STAT3 in anti-apoptosis. Immunity, 1996;5:449–60.

8. Ihara S, Nakajima K, Fukada T, et al. Dual control of neurite outgrowth by STAT3 and MAP kinase in PC12 cells stimulated with interleukin-6. EMBO J, 1997;16:5345–52.

9. Bromberg J, Darnell JE Jr. The role of STATs in transcriptional control and their impact on cellular function. Oncogene, 2000;19:2468–73.

10. Buettner R, Mora LB, Jove R. Activated STAT signaling in human tumors provides novel molecular targets for therapeutic intervention. Clin Cancer Res, 2002;8:945–54.

11. Bowman T, Garcia R, Turkson J, Jove R. STATs in oncogenesis. Oncogene, 2000;19:2474–88.

12. Bromberg JF, Wrzeszczynska MH, Devgan G, et al. Stat3 as an oncogene. Cell, 1999;98:295–303.

13. Grandis JR, Drenning SD, Chakraborty A, et al. Requirement of Stat3 but not Stat1 activation for epidermal growth factor receptor-mediated cell growth *in vitro*. J Clin Invest, 1998;102:1385–92.

14. Turkson J, Ryan D, Kim JS, et al. Phosphotyrosyl peptides block Stat3 mediated DNA binding activity, gene regulation, and cell transformation. J Biol Chem, 2001;276:45443–55.

15. Ren Z, Cabell LA, Schaefer TS, McMurray JS. Identification of a high-affinity phosphopeptide inhibitor of Stat3. Bioorg Med Chem Lett, 2003;13:633–6.

16. Catlett-Falcone R, Landowski TH, Oshiro MM, et al. Constitutive activation of Stat3 signaling confers resistance to apoptosis in human U266 myeloma cells. Immunity, 1999;10:105–15.

17. Niu G, Heller R, Catlett-Falcone R, et al. Gene therapy with dominant-negative Stat3 suppresses growth of the murine melanoma B16 tumor *in vivo*. Cancer Res, 1999;59:5059–63.

18. Garcia R, Bowman TL, Niu G, et al. Constitutive activation of Stat3 by the Src and JAK tyrosine kinases participates in growth regulation of human breast carcinoma cells. Oncogene, 2001;20:2499–513.

19. Wei D, Le X, Zheng L, et al. Stat3 activation regulates the expression of vascular endothelial growth factor and human pancreatic cancer angiogenesis and metastasis. Oncogene, 2003;22:319–29.

20. Blaskovich MA, Sun J, Cantor A, Turkson J, Jove R, Sebti SM. Discovery of JSI-124 (cucurbitacin I), a selective Janus kinase/signal transducer and activator of transcription 3 signaling pathway inhibitor with potent antitumor activity against human and murine cancer cells in mice. Cancer Res, 2003;63:1270–9.

21. Niu G, Shain KH, Huang M, et al. Overexpression of a dominant-negative signal transducer and activator of transcription 3 variant in tumor cells leads to production of soluble factors that induce apoptosis and cell cycle arrest. Cancer Res, 2001;61:3276–80.

22. Ivanov VN, Bhoumik A, Krasilnikov M, et al. Cooperation between STAT3 and c-*jun* suppresses Fas transcription. Mol Cell, 2001;7:517–28.

23. Epling-Burnette PK, Liu JH, Catlett-Falcone R, et al. Inhibition of STAT3 signaling leads to apoptosis of leukemic large granular lymphocytes and decreased Mcl-1 expression. J Clin Invest, 2001;107:351–62.

24. Mai JC, Mi Z, Kim SH, Ng B, Robbins PD. A proapoptotic peptide for the treatment of solid tumors. Cancer Res, 2001;61:7709–12.

25. Asoh S, Ohsawa I, Mori T, et al. Protection against ischemic brain injury by protein therapeutics. Proc Natl Acad Sci USA, 2002;99:17107–12.

26. de Soultrait VR, Desjobert C, Tarrago-Litvak L. Peptides as new inhibitors of HIV-1 reverse transcriptase and integrase. Curr Med Chem, 2003;10:1765–78.

27. Schwarze SR, Dowdy SF. *in vivo* protein transduction: intracellular delivery of biologically active proteins, compounds and DNA. Trends Pharmacol Sci, 2000;21:45–8.

28. Wender PA, Mitchell DJ, Pattabiraman K, Pelkey ET, Steinman L, Rothbard JB. The design, synthesis, and evaluation of molecules that enable or enhance cellular uptake: peptoid molecular transporters. Proc Natl Acad Sci USA, 2000;97:13003–8.

29. Futaki S, Suzuki T, Ohashi W, et al. Arginine-rich peptides. An abundant source of membrane-permeable peptides having potential as carriers for intracellular protein delivery. J Biol Chem, 2001;276:5836–40.

30. Matsui H, Tomizawa K, Lu YF, Matsushita M. Protein Therapy: *in vivo* protein transduction by polyarginine (11R) PTD and subcellular targeting delivery. Curr Protein Peptide Sci, 2003;4:151–7.

31. Williams EJ, Dunican DJ, Green PJ, et al. Selective inhibition of growth factor-stimulated mitogenesis by a cell-permeable Grb2-binding peptide. J Biol Chem, 1997;272:22349–54.

32. Schwarze SR, Ho A, Vocero-Akbani A, Dowdy SF. *in vivo* protein transduction: delivery of a biologically active protein into the mouse. Science, 1999;285:1569–72.

33. Zolotarevsky Y, Hecht G, Koutsouris A, et al. A membrane-permeant peptide that inhibits MLC kinase restores barrier function in *in vitro* models of intestinal disease. Gastroenterology, 2002;123:163–72.

34. Buerger C, Nagel-Wolfrum K, Kunz C, et al. Sequence-specific peptide aptamers, interacting with the intracellular domain of the epidermal growth factor receptor, interfere with Stat3 activation and inhibit the growth of tumor cells. J Biol Chem, 2003;278:37610–21.

35. Fulda S, Wick W, Weller M, Debatin KM. Smac agonists sensitize for Apo2L/T. Nat Med, 2002;8:808–15.

36. Butz K, Denk C, Ullmann A, Scheffner M, Hoppe-Seyler F. Induction of apoptosis in human papillomavirus positive cancer cells by peptide aptamers targeting the viral E6 oncoprotein. Proc Natl Acad Sci USA, 2000;97:6693–7.

37. Ladner RC. Constrained peptides as binding entities. Trends Biotechnol, 1995;13:426–30.

38. Hoppe-Seyler F, Butz K. Peptide aptamers: powerful new tools for molecular medicine. J Mol Med, 2000;78:426–30.

39. Hoppe-Seyler F, Crnkovic-Mertens I, Denk C, et al. Peptide aptamers: new tools to study protein interactions. J Steroid Biochem Mol Biol, 2001;78:105–11.

40. Colas P, Cohen B, Jessen T, Grishina I, McCoy J, Brent R. Genetic selection of peptide aptamers that recognize and inhibit cyclin-dependent kinase 2. Nature, 1996;380:548–50.

41. Cohen BA, Colas P, Brent R. An artificial cell-cycle inhibitor isolated from a combinatorial library. Proc Natl Acad Sci USA, 1998;95:14272–7.

42. Kolonin MG, Finley RL Jr. Targeting cyclin-dependent kinases in *Drosophila* with peptide aptamers. Proc Natl Acad Sci USA, 1998;95:14266–71.

43. Fabbrizio E, Le Cam L, Polanowska J, et al. Inhibition of mammalian cell proliferation by genetically selected peptide aptamers that functionally antagonize E2F activity. Oncogene, 1999;18:4357–63.

44. Butz K, Denk C, Fitscher B, et al. Peptide aptamers targeting the hepatitis B virus core protein: a new class of molecules with antiviral activity. Oncogene, 2001;20:6579–86.

45. Nauenburg S, Zwerschke W, Jansen-Durr P. Induction of apoptosis in cervical carcinoma cells by peptide aptamers that bind to the HPV-16 E7 oncoprotein. FASEB J, 2001;15:592–4.

46. Oshiro MM, Landowski TH, Catlett-Falcone R, et al. Inhibition of JAK kinase activity enhances Fas-mediated apoptosis but reduces cytotoxic activity of topoisomerase II inhibitors in U266 myeloma cells. Clin Cancer Res, 2001;7:4262–71.

47. Darnell JE Jr. STATs and gene regulation. Science, 1997;277:1630–5.

48. Becker S, Groner B, Muller CW. Three-dimensional structure of the Stat3β homodimer bound to DNA. Nature, 1998;394:145–51.

49. Di Fiore PP, Pierce JH, Fleming TP, et al. Overexpression of the human EGF receptor confers an EGF-dependent transformed phenotype to NIH 3T3 cells. Cell, 1987;51:1063–70.

50. Biscardi JS, Tice DA, Parsons SJ. c-Src, receptor tyrosine kinases, and human cancer. Adv Cancer Res, 1999;76:61–119.

51. Garcia R, Yu CL, Hudnall A, et al. Constitutive activation of Stat3 in fibroblasts transformed by diverse oncoproteins and in breast carcinoma cells. Cell Growth & Differ, 1997;8:1267–76.

52. Olayioye MA, Neve RM, Lane HA, Hynes NE. The ErbB signaling network: receptor heterodimerization in development and cancer. EMBO J, 2000;19:3159–67.

53. Cory S, Adams JM. The Bcl2 family: regulators of the cellular life-or-death switch. Nat Rev Cancer, 2002;2:647–56.

54. Reed JC. Mechanisms of apoptosis. Am J Pathol, 2000;157:1415–30.

55. Patel T, Gores GJ, Kaufmann SH. The role of proteases during apoptosis. FASEB J, 1996;10:587–97.

56. Chene P. Inhibiting the p53-MDM2 interaction: an important target for cancer therapy. Nat Rev Cancer, 2003;3:102–9.

57. Herr I, Debatin KM. Cellular stress response and apoptosis in cancer therapy. Blood, 2001;98:2603–14.

58. Ivanov VN, Bhoumik A, Ronai Z. Death receptors and melanoma resistance to apoptosis. Oncogene, 2003;22:3152–61.

59. Walczak H, Krammer PH. The CD95 (APO-1/Fas) and the TRAIL (APO2L) apoptosis systems. Exp Cell Res, 2000;256:58–66.

60. Reed JC. Bcl-2 family proteins. Oncogene, 1998;17:3225–36.

61. Debatin KM, Poncet D, Kroemer G. Chemotherapy: targeting the mitochondrial cell death pathway. Oncogene, 2002;21:8786–803.

62. Dole MG, Jasty R, Cooper MJ, Thompson CB, Nunez G, Castle VP. Bcl-x_L is expressed in neuroblastoma cells and modulates chemotherapy-induced apoptosis. Cancer Res, 1995;55:2576–82.

63. Smythe WR, Mohuiddin I, Ozveran M, Cao XX. Antisense therapy for malignant mesothelioma with oligonucleotides targeting the Bcl-x_L gene product. J Thorac Cardiovasc Surg, 2002;123:1191–8.

64. Degterev A, Lugovskoy A, Cardone M, et al. Identification of small-molecule inhibitors of interaction between the BH3 domain and Bcl-x_L. Nat Cell Biol, 2001;3:173–82.

65. Tzung SP, Kim KM, Basanez G, et al. Antimycin A mimics a cell-death-inducing Bcl-2 homology domain 3. Nat Cell Biol, 2001;3:183–91.

66. Simoes-Wust AP, Olie RA, Gautschi O, et al. Bcl-x_L antisense treatment induces apoptosis in breast carcinoma cells. Int J Cancer, 2000;87:582–90.

67. Leech SH, Olie RA, Gautschi O, et al. Induction of apoptosis in lung-cancer cells following Bcl-x_L anti-sense treatment. Int J Cancer, 2000;86:570–6.

68. Niesner U, Halin C, Lozzi L, et al. Quantitation of the tumor-targeting properties of antibody fragments conjugated to cell-permeating HIV-1 TAT peptides. Bioconjug Chem, 2002;13:729–36.

69. Cao G, Pei W, Ge H, et al. *in vivo* delivery of a Bcl-x_L fusion protein containing the TAT protein transduction domain protects against ischemic brain injury and neuronal apoptosis. J Neurosci, 2002;22:5423–31.

70. Schmidt M, Maurer-Gebhard M, Groner B, Kohler G, Brochmann-Santos G, Wels W. Suppression of metastasis formation by a recombinant single chain antibody-toxin targeted to full-length and oncogenic variant EGF receptors. Oncogene, 1999;18:1711–21.

71. Haque SJ, Wu Q, Kammer W, et al. Receptor-associated constitutive protein tyrosine phosphatase activity controls the kinase function of JAK1. Proc Natl Acad Sci USA, 1997;94:8563–8.

72. Wolfrum U. Centrin in the photoreceptor cells of mammalian retinae. Cell Motil Cytoskeleton, 1995;32:55–64.

Molecular Cancer Research

The Interaction of Specific Peptide Aptamers With the DNA Binding Domain and the Dimerization Domain of the Transcription Factor Stat3 Inhibits Transactivation and Induces Apoptosis in Tumor Cells [1]

1Deutsche Krebshilfe, Dr. Mildred Scheel Stiftung für Krebsforschung, Bonn (10-1626-Gr2), and Novartis Stiftung für Therapeutische Forschung.

Kerstin Nagel-Wolfrum, Claudia Buerger, Ilka Wittig, et al.

Mol Cancer Res 2004;2:170-182.